

ARTICLE TYPE**An X-ray View of the Hot Circum-Galactic Medium[†]**Jiang-Tao Li^{1,*}¹Department of Astronomy, University of Michigan, MI, U.S.A.**Correspondence**

*Jiang-Tao Li, 311 West Hall, 1085 S. University Ave, Ann Arbor, MI, 48109-1107. Email: pandataotao@gmail.com

Present Address

311 West Hall, 1085 S. University Ave, Ann Arbor, MI, 48109-1107

Funding Information

National Aeronautics and Space Administration (NASA), 80NSSC19K0579. 80NSSC18K0536. 80NSSC19K1013. Smithsonian Institution, AR9-20006X.

The hot circum-galactic medium (CGM) represents the hot gas distributed beyond the stellar content of the galaxies while typically within their dark matter halos. It serves as a depository of energy and metal-enriched materials from galactic feedback and a reservoir from which the galaxy acquires fuels to form stars. It thus plays a critical role in the coevolution of galaxies and their environments. X-rays are one of the best ways to trace the hot CGM. I will briefly review what we have learned about the hot CGM based on X-ray observations over the past two decades, and what we still do not know. I will also briefly prospect what may be the foreseeable breakthrough in the next one or two decades with future X-ray missions.

KEYWORDS:

galaxies: evolution, galaxies: halos, (galaxies:) intergalactic medium, galaxies: statistics, X-rays: galaxies

1 | WHAT WE ALREADY KNOW ABOUT THE HOT CGM?

The hot circum-galactic medium (CGM), or sometimes named as the galactic corona, represents X-ray emitting hot gas typically at a temperature of $kT \sim 10^{6-8}$ K around galaxies. The hot CGM could extend beyond the galaxy stellar disk and bulge and typically out to the virial radius of the dark matter halo or even beyond (Fig. 1 a,b). In principle, the hot CGM could cool and fall back onto the galaxy, providing fresh fuel to continue star formation. It can also be ejected out of the galaxy, entraining a lot of energy and metal-enriched material from galactic stellar (stellar wind, supernovae: SNe, etc.) or AGN feedback.

1.1 | Key science related to the hot CGM

As probably the most spatially extended and volume filling phase of the CGM, the hot gas could be important in the coevolution of galaxies and their environments, in particular, in the mass and energy budgets of the galaxies.

The hot CGM could contain a significant fraction of the “missing baryons” (e.g., Anderson & Bregman 2010;

Bregman 2007; Bregman et al. 2018). As the soft X-ray emission from hot gas is dominated by metal lines whose strength is proportional to both the gas density and metallicity, the detected soft X-ray emission around nearby galaxies is largely biased to the highly metal enriched CGM around actively star forming (SF) galaxies. This part dominates the X-ray emission but may contain only a small fraction of the baryon mass (e.g., Crain et al. 2013). In order to measure the total mass contained in the extended hot CGM, we need to detect the hot gas at large galacto-centric radii where the feedback material encounters the metal-poor gas accreted from outside the galaxies (e.g., Benson et al. 2000; Toft et al. 2002). Since L^* [an L^* galaxy has a roughly comparable optical luminosity as the Milky Way (MW)] or sub- L^* galaxies are not massive enough to gravitationally heat the gas to X-ray emitting temperature, while massive elliptical galaxies are often located in clusters, the best candidates to search for the accreted and gravitationally heated hot CGM would be massive disk galaxies. There are many efforts searching for the extended hot CGM around such galaxies (e.g., Anderson & Bregman 2011; Anderson et al. 2013; Bogdán et al. 2013,1,1; Dai et al. 2012; Li et al. 2016b,1; Rasmussen et al. 2009), while the latest efforts indicates that even in these most massive and isolated systems, the hot CGM may not be sufficient to account for the “missing baryons” (Fig. 1 c; Li et al. 2018).

[†]An X-ray View of the Hot Circum-Galactic Medium⁰Abbreviations: X-ray View of the hot CGM

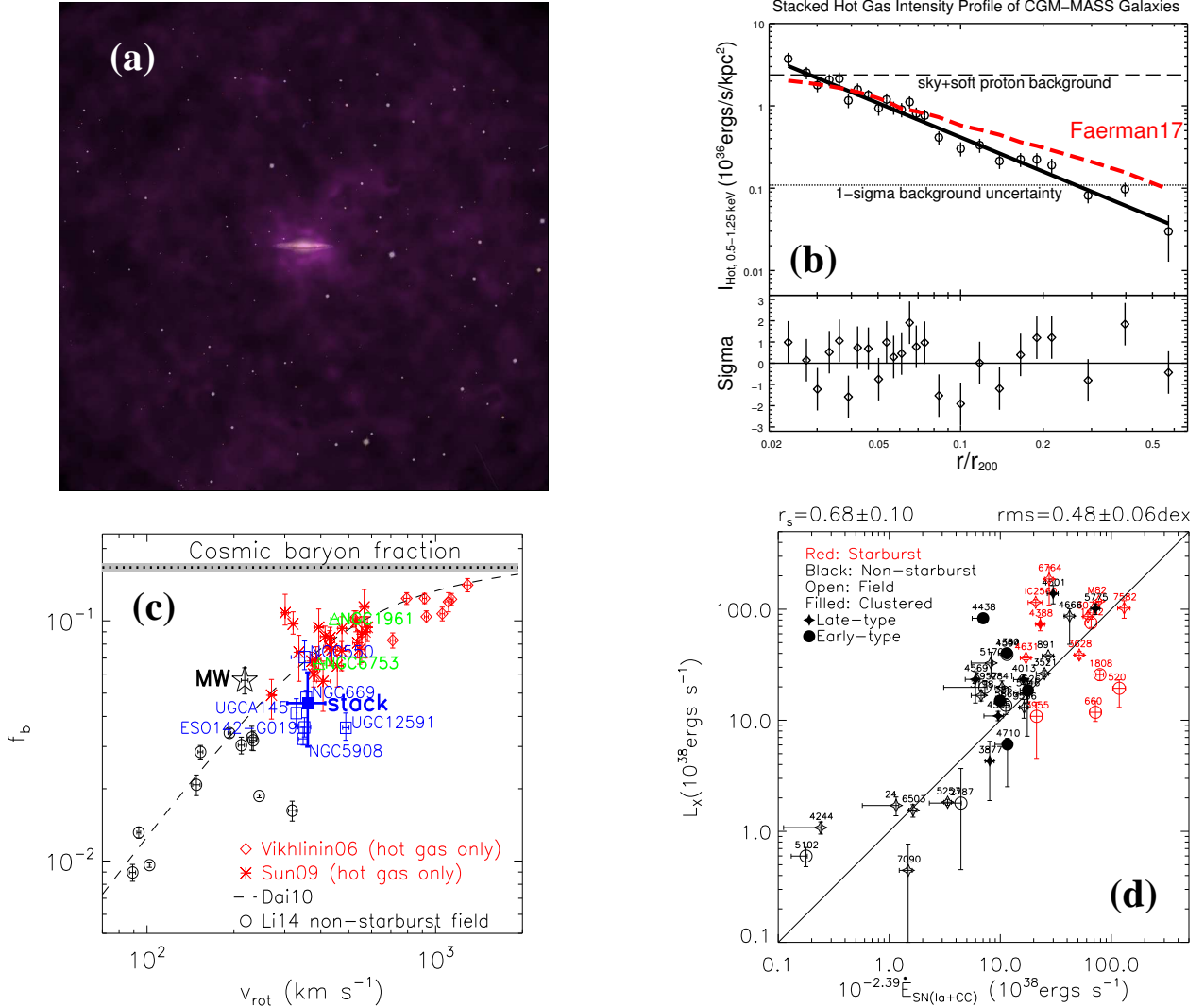


FIGURE 1 (a) Stacked diffuse soft X-ray images of the CGM-MASS galaxies (purple; from ESA press release, with original data from Li et al. 2018) overlaid on the SDSS image of NGC 5908 (white). (b) Stacked radial intensity profiles of the hot gas component of the CGM-MASS galaxies (Li et al., 2018). The radial distance of different galaxies has been rescaled to r_{200} . The solid line is the best-fit β -function. The dashed and dotted lines show the sky+soft proton background and the 1σ uncertainty. The red dashed curve is the Faerman et al. (2017) model scaled with r_{200} of a MW-sized halo. (c) Baryon fraction (f_b) v.s. rotation velocity (v_{rot}) (Li et al., 2018). The cosmic baryon fraction (dotted line) with error (shaded area), a fitted relation from Dai et al. (2010) (dashed), the MW (Miller & Bregman 2015; black star), samples of non-starburst field spirals (Li et al. 2014; black circles), galaxy groups (Sun et al. 2009; red stars), and galaxy clusters (Vikhlinin et al. 2006; red diamonds) are plotted for comparison. (d) L_X v.s. the total SN energy injection rate $\dot{E}_{\text{SN}(\text{CC}+\text{Ia})}$ fitted with a linear relation (Li & Wang, 2013b).

The hot CGM could also contain a significant fraction of the energy injected by various types of galactic feedback (e.g., Li & Wang 2013b). This gas phase could contain energy at least in a few forms such as radiative loss, kinetic energy of global motion, and turbulent energy. We herein consider the global energy budget of galaxies with a few simplified assumptions. We do not consider *AGN feedback* as it is the most important in very massive systems and on large scales (e.g., for the intracluster medium ICM), and may not have continuous

energy injection over the lifetime of galaxies. Most of the CGM phases are detected typically at $r < 20 \text{ kpc}$ (e.g., Li & Wang 2013a), where *gravitational heating* is typically not as important as feedback. As most of the energy input from *young stars* (radiation, stellar wind, etc.) is reprocessed by the ISM locally near SF regions and the CGM is optically thin to the reprocessed emission (peaked in infrared), stars do not contribute much to the global energy balance of the CGM. Therefore, in the simplest case, we only consider *energy injection from SNe*

TABLE 1 Measured SNe Energy Budget in the CGM.

Phase	Fraction	Reference
Thermal energy of hot gas radiated in X-ray	$\sim 1\% \dot{E}_{\text{SN}}$	Li & Wang (2013b)
Kinetic energy of the global motion of hot gas	$\lesssim 1\% \dot{E}_{\text{SN}}$	Li & Wang (2013b) ¹
Turbulent energy of small-scale motion of hot gas	$\lesssim 0.1\% \dot{E}_{\text{SN}}$	Hitomi (2016) ²
Kinetic energy of cold gas outflow	$< 1\% \dot{E}_{\text{SN}}$	Contursi et al. (2013)
Radiative cooling of cool gas	$\lesssim 5\% \dot{E}_{\text{SN}}$	Otte et al. (2003)
Cosmic ray	$\sim 5\% \dot{E}_{\text{SN}}$	Li et al. (2016a) ³
Magnetic field	$< 5\% \dot{E}_{\text{SN}}$	Mora-Partiarroyo et al. (2019)
Total CGM	$< 20\% \dot{E}_{\text{SN}}$	-

A rough estimate of the fraction of SNe energy injection rate (\dot{E}_{SN}) distributed into different phases of the CGM. Other energy sources (AGN, gravitational heating, stellar radiation and wind, etc.) and the energy consumed locally in the ISM are not included here. The estimates are made based on different samples (many are just case studies) and different assumptions.

1. Estimated assuming a pressure driven adiabatic expansion.
 2. Estimated assuming the same turbulent to thermal pressure ratio as in the Perseus cluster.

3. Estimated assuming a typical CR hadron-to-lepton energy density ratio of 50 (Strong et al., 2010).

and compare it to the *energy detected in various CGM phases*. Table 1 summarizes a very rough estimate of the SNe energy budget in the CGM. We emphasize that reliable observations of many CGM phases are still very limited, so the numbers in Table 1 are just order of magnitude estimate with very different samples (many are just case studies) and often highly uncertain assumptions. The basic conclusion is that a significant fraction of SNe energy is not detected around galaxies, which is often regarded as the “missing galactic feedback” problem (e.g., Wang 2010). Such a problem is also revealed by the lack of heavy elements from feedback in the CGM (e.g., Wang 2010).

1.2 | Detection and statistics of the extended X-ray emission around nearby galaxies

Extended soft X-ray emission, which is often thought to be largely contributed, if not dominated by hot gas, has been commonly detected around various types of nearby galaxies. The detection, however, is often limited to a few tenth of kpc from the galactic center around isolated galaxies

(e.g., Bogdán et al. 2015; Kim et al. 2019; Li & Wang 2013a; Strickland et al. 2004a; Tüllmann et al. 2006a). Apparent scaling relations between the X-ray properties of the “hot CGM” and various galaxy parameters have been well established in many existing works (e.g., Fig. 1 d; Boroson et al. 2011; Kim & Fabbiano 2013; Li & Wang 2013b; Mineo et al. 2014; O’Sullivan et al. 2003; Strickland et al. 2004b; Tüllmann et al. 2006b; Wang et al. 2016). Most of these scaling relations indicate that the soft X-ray emissions around galaxies are connected to the stellar feedback activities in the galaxies, but different types of galaxies have clearly different X-ray properties and scaling relations. In general, in addition to core collapsed SNe which are related to the young stellar population, Type Ia SNe related to the relatively old stellar population could also be important, especially in early-type galaxies (e.g., Li 2015). On the other hand, gravitational heating, which could be important in massive isolated galaxies, has been suggested but not yet firmly evidenced based on existing observations (e.g., Li et al. 2017).

2 | WHAT WE STILL DON’T KNOW?

2.1 | What are the physical, chemical, and dynamical properties of the hot CGM?

In addition to thermal plasma, the soft X-ray emission around nearby galaxies could also be contributed by other non-thermal components. One of the most important non-thermal components is charge exchange (CX), which is characterized with a few soft X-ray emission lines (e.g., Smith et al. 2012) and has been evidenced with high resolution grating spectra of the diffuse soft X-ray emission around a few nearby galaxies (e.g., Fig. 2 a; Liu et al. 2011,1; Ranalli et al. 2008). CX could be important or even dominant in some cases. However, in most of the X-ray observations of nearby galaxies, the low resolution CCD spectra prevent us from separating the CX from the thermal plasma component. Even if most of the detected soft X-ray emission is produced by the hot plasma, the thermal structure of gas can be complicated (e.g., Hodges-Kluck et al. 2018) and it is often difficult to decompose different gas components (at different temperature and density) with the existing CCD imaging spectroscopy observations (e.g., Li & Wang 2013a).

The importance of CX indicates that there is a strong cool-hot gas interaction in nearby galaxies. A very hot and tenuous gas component therefore highly likely exists and could be produced by the thermalized SNe ejecta (e.g., Strickland et al. 2002; Tang et al. 2009). This gas component has too low density and X-ray emissivity, and the best tracer of it is the Fe K shell emission lines at 6 – 7 keV. Strickland & Heckman (2007,0) claimed the detection of ionized Fe K line in the nuclear region of M82, which is the most solid such detections

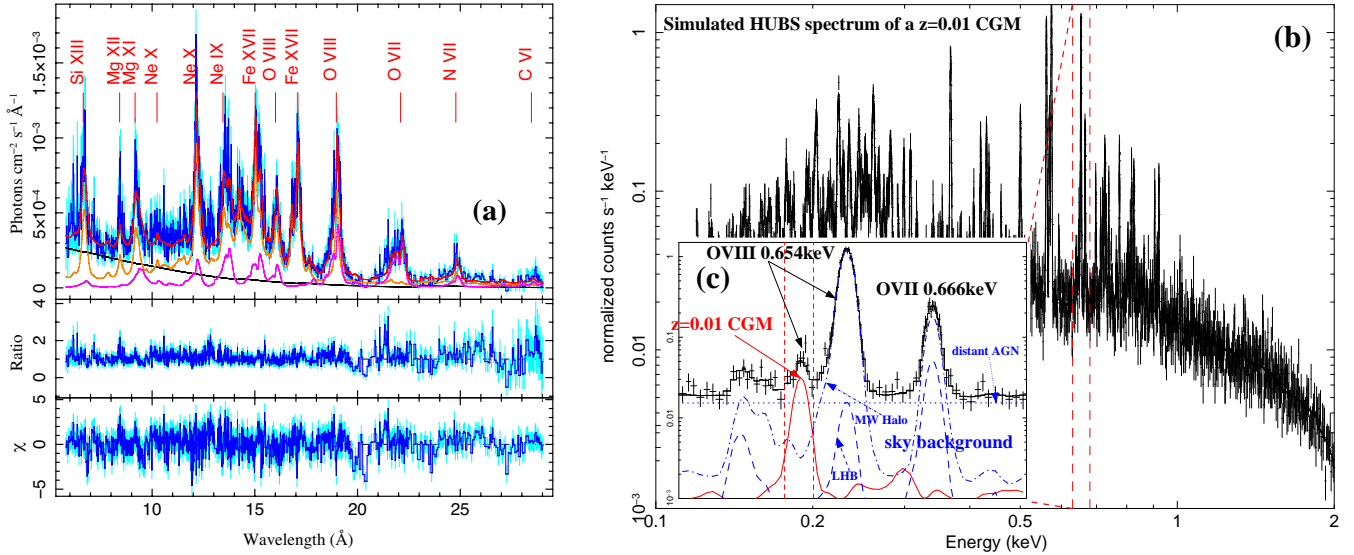


FIGURE 2 (a) XMM-Newton/RGS spectrum of M82 and the best-fit model [red curve; different components in different colors: power law (black), thermal (orange), CX (purple); Zhang et al. 2014]. (b) Simulated 1 Ms HUBS spectrum of the hot CGM at $r \leq 0.2 r_{200}$ around a $z = 0.01$ ($d \sim 50$ Mpc) galaxy (e.g., NGC 5908, Table 3 ; Li et al. 2016b). (c) Zoom-in of panel (b) in 0.63–0.68 keV. The red curve is the hot CGM (0.6 keV plasma), while the blue curves are various sky background components (local hot bubble LHB; MW halo; distant AGN). The redshifted OVIII line from the CGM can be separated from the background.

so far, but the detection may be highly contaminated by stellar sources (e.g., Revnivtsev et al. 2009). Therefore, there is still no direct evidence on the existence of such a hot gas component, and its physical and chemical parameters, as well as the related cool-hot gas interactions, are still poorly understood.

Even if we can assume thermal origin of the X-ray emission, the chemical and dynamical properties of the hot CGM are still poorly constrained, based on the low-resolution CCD spectra. It is therefore difficult to measure the amount of heavy elements and kinetic/turbulent energy contained in the hot CGM. Furthermore, because in the modeling of the low-resolution X-ray spectra, the emission measure (or gas density) is degenerated with the metallicity, the measured gas density and mass also have large uncertainties (e.g., Bogdán et al. 2013; Li et al. 2016b). These uncertainties strongly affect our understanding of the metal, energy, and baryon budget of the hot CGM.

2.2 | Hot gas distribution at large radii

Radial distribution of the hot CGM around galaxies is often poorly constrained at large galacto-centric radii because of the low density thus X-ray emissivity of the hot gas. Furthermore, in broad-band imaging observations, the detection limit of faint extended features is limited by the uncertainty of the background, instead of the depth of the observations (Fig. 1 b). Therefore, the hot CGM around individual isolated galaxies, even the most massive ones, is typically detected to $r \lesssim 50$ kpc, or $\sim (10 - 20)\% r_{200}$ (e.g., Bogdán et al. 2013; Dai et al. 2012;

Li et al. 2017). At this radius, the radial distribution of the hot CGM could still be highly affected by galactic feedback. It is therefore difficult to distinguish different models based on the directly measured hot gas radial distribution (Fig. 1 b).

Furthermore, because the origin of gas at larger radii may be quite different (more gas with external instead of internal origin thus lower metallicity), the poor constraint of gas distribution at $r \gtrsim (10 - 20)\% r_{200}$ prevents us from both searching for the accreted hot CGM and measuring the total mass and energy contained in the CGM. It is not impossible that the hot CGM extends beyond the virial radius of the dark matter halo thus contains a larger fraction of the missing baryons (Bregman et al., 2018), but better observations are needed to constrain the hot gas distribution at large radii.

3 | WHAT CAN WE DO IN THE FUTURE?

3.1 | Future focusing X-ray telescopes

In the next 10-20 years, there are a few focusing soft X-ray telescopes either already approved or currently in concept study. Most of these telescopes have higher energy resolution and/or better sensitivity than the existing X-ray missions, thus could potentially improve our understanding of the hot CGM. Table 2 summarizes basic parameters of these future X-ray missions in comparison with some existing ones.

For a quantitative comparison among these X-ray missions in the study of the hot CGM, we calculate the Figure-of-Merit

TABLE 2 FoM of Some Current and Future X-ray Missions.

Mission	$E/\Delta E$ †	$A_{\text{eff}}/\text{cm}^2$	$\Omega_{\text{FOV}}/\text{deg}^2$	FoM
Chandra/ACIS-I	10	110	0.079	87
XMM-Newton/EPIC‡	15	1000	0.25	3750
Suzaku/XIS	10	1000	0.09	900
eROSITA	10	1000	1.0	10000
XRISM	100	70	0.0023	22
Athena/X-IFU	240	5000	0.0069	8280
Lynx	200	10000	0.0069	13800
HUBS	300	500	1.0	150000
AXIS	10	7000	0.05	3500
Super-DIOS	300	1000	0.25	75000

FoM of a few current and future focusing X-ray telescopes for emission line detections of extended sources. Parameters are mostly obtained from the website of each mission.

†Energy resolution $E/\Delta E$ and effective area A_{eff} are typical values in soft X-ray (~ 1 keV).

‡For a combination of PN + 2 MOS CCDs.

(FoM) for emission line detections of extended sources for the major instrument of each mission, which is defined as:

$$FoM = RA_{\text{eff}}\Omega_{\text{FOV}}, \quad (1)$$

where R is the energy resolution in $E/\Delta E$, A_{eff} is the effective area in cm^2 , and Ω_{FOV} is the field of view (FOV) in deg^2 . The FoM describes the efficiency of an instrument in detecting soft X-ray emission lines from extended sources.

Many future X-ray missions have significantly improved energy resolution in imaging spectroscopy mode with the micro-calorimeter detector in replacement of CCD (McCammon 2005; e.g., XRISM, Athena, Lynx, HUBS, and Super-DIOS). The most direct effect is the significantly higher FoM than CCD X-ray missions (Table 2). In particular, also with their large FOVs, HUBS and Super-DIOS will be the most efficient instruments in detecting the extended hot CGM around local galaxies, although as small missions, their effective areas are not superb (Cui et al., 2019; Yamada et al., 2018). Angular resolution is not as important as in the study of point-like sources, because point source contributions (stellar sources, AGN) can always be well removed in spectral space, especially in narrow-band.

3.2 | Science with future X-ray missions

With the significantly improved energy resolution in imaging spectroscopy mode, we expect to have some breakthrough on the study of the hot CGM with some future X-ray missions.

- **Nature of soft X-ray emission.** Diagnostic emission line features (e.g., the resonance, intercombination, and forbidden lines of the OVII $K\alpha$ triplet) can only be resolved with high resolution X-ray spectra (e.g., with $E/\Delta E \gtrsim 100$). These lines play a key role in determining the nature of the soft X-ray emission, i.e., if it is produced by thermal plasma or any non-thermal processes such as CX (e.g., Zhang et al. 2014). The required resolution can be achieved with existing X-ray grating spectra (e.g., XMM-Newton/RGS) which has been less commonly adopted in the study of extended sources (the lines can be significantly broadened because of blending of emission from different parts of the extended source, e.g., Fig. 2 a). In the future, with more micro-calorimeter observations, we will be able to more accurately decompose the soft X-ray emission and determine its nature in more galaxies.
- **Metallicity of hot gas.** A reliable measurement of gas metallicity in X-ray in principle requires the separation of the lines and the continuum. In CCD spectra the lines and continuum are mixed together, so in spectral modeling the metallicity and gas density are degenerated and cannot be well constrained simultaneously. Most of the existing metallicity measurements are highly model dependent and uncertain, and usually only some abundance ratios are reliable (e.g., O/Fe; Li 2015). The condition can be significantly improved with micro-calorimeter.
- **Dynamics of hot gas.** We need a velocity resolution of $\sim 10^3$ km s $^{-1}$ (or $E/\Delta E \sim 300$) to measure a line shift or broadening as small as (200–300) km s $^{-1}$. This is the typical value of a moderate gas outflow (or global inflow) in a non-starburst galaxy, especially for the soft X-ray emitting gas which may be largely produced at the interface between the wind fluid and the entrained cool gas. We could thus be able to estimate the kinetic and turbulent energy contained in the hot CGM.
- **Detection of extended CGM with narrow-band imaging.** In the study of hot CGM, we are mostly interested in a few diagnostic lines such the OVIII line at ~ 0.65 keV. In slightly redshifted galaxies, these lines can be separated from the same lines produced by the MW halo (the most important background component limiting the detection). Therefore, with high enough spectral resolution, we can conduct narrow-band imaging only including these lines, in order to achieve a much lower background and detection surface brightness. We did a simple simulation with the HUBS response files to show the basic concept of this method (Fig. 2 b,c). We also have a rough estimate of the requested energy resolution for a few local objects at different redshifts (Table 3). As the hot CGM is very faint and cannot be detected around too distant galaxies (e.g.,

TABLE 3 Parameters of Local Objects Which May Be Used for Narrow-band Imaging Observations.

Object	d/Mpc	$v_{\odot}/\text{km s}^{-1}$	$r_{\text{virial}}/\text{deg}$	$\Delta E/\text{eV}$
NGC891	10	530	1.5	1
Virgo Cluster	16	1280	4	2.5
Fornax Cluster	20	1340	1.9	2.7
NGC5908	50	3300	0.5	6.5
Perseus Cluster	75	5400	1.3	10
Coma Cluster	100	6900	1.5	14

v_{\odot} is the heliocentric receding velocity. r_{virial} is the apparent virial radius of the dark matter halo in degree. ΔE is the requested energy resolution to separate emission lines from the CGM of redshifted objects and the MW halo at ~ 0.6 keV.

with $d \gtrsim 100$ Mpc), an energy resolution of $(1 - 2)$ eV is required for the study of local galaxies at $d \lesssim 20$ Mpc (e.g., the Virgo cluster galaxies). In this case, a large FOV (typically \sim degree) is needed to cover a large fraction of the dark matter halo. This is why HUBS and Super-DIOS will be the best for narrow-band imaging observations of the hot CGM.

In addition to the significantly improved spectral resolution, the *survey capability* of some missions (e.g., eROSITA) will also be very helpful in the study of hot CGM. This is not only for statistical analysis of large samples comparing the properties of different galaxy subsamples, but also help us to conduct stacking analysis probing the spatial distribution of faint extended hot CGM (e.g., Anderson et al. 2013; Li et al. 2018). Furthermore, we only discussed the X-ray emission line observations of the hot CGM, but the hot CGM can also be studied via *absorption lines of background AGN*, or *SZ effects*.

ACKNOWLEDGMENTS

JTL acknowledge Dr. Shuinai Zhang to provide Fig. 2 a and the financial support from the **National Aeronautics and Space Administration (NASA)** through the grants *80NSSC19K0579*, *80NSSC18K0536*, *80NSSC19K1013*, and the **Smithsonian Institution** through the grants *AR9-20006X*.

REFERENCES

- Anderson M. E., Bregman J. N., 2010, ApJ, 714, 320
 Anderson M. E., Bregman J. N., 2011, ApJ, 737, 22
 Anderson M. E., Bregman J. N., Dai X., 2013, ApJ, 762, 106
 Benson A. J., Bower R. G., Frenk C. S., White S. D. M., 2000, MNRAS, 314, 557
 Bogdán A., Forman W. R., Vogelsberger M., et al., 2013, ApJ, 772, 97
 Bogdán A., Vogelsberger M., Kraft R. P., et al., 2015, ApJ, 804, 72
 Bogdán A., Bourdin H., Forman W. R., Kraft R. P., Vogelsberger M., Hernquist L., Springel V., 2017, ApJ, 850, 98
 Bregman J. N., 2007, ARA&A, 45, 221
 Bregman J. N., Anderson M. E., Miller M. J., et al., 2018, ApJ, 862, 3
 Boroson B., Kim D.-W., Fabbiano G., 2011, ApJ, 729, 12
 Contursi A., Poglitsch A., Graciá C. J., et al., 2013, A&A, 549, 118
 Crain R. A., McCarthy I. G., Schaye J., Theuns T., Frenk C. S., 2013, MNRAS, 432, 3005
 Cui W., Chen L.-B., Gao B., et al., 2019, submitted to JLTTP.
 Dai X., Bregman J. N., Kochanek C. S., Rasia E., 2010, ApJ, 719, 119
 Dai X., Anderson M., Bregman J., Miller J. M., 2012, ApJ, 755, 107
 Faerman Y., Sternberg A., McKee C. F., 2017, ApJ, 835, 52
 Hitomi Collaboration, 2016, Nature, 535, 117
 Hodges-Kluck E. J., Bregman J. N., Li J.-t., 2018, ApJ, 866, 126
 Kim D.-W., Fabbiano G., 2013, ApJ, 776, 116
 Kim D.-W., Anderson C., Burke D., et al., 2019, ApJS, 241, 36
 Li J.-T., Wang Q. D., 2013a, MNRAS, 428, 2085
 Li J.-T., Wang Q. D., 2013b, MNRAS, 435, 3071
 Li J.-T., Crain R. A., Wang Q. D., 2014, MNRAS, 440, 859
 Li J.-T., 2015, MNRAS, 453, 1062
 Li J.-T., Beck R., Dettmar R.-J., et al., 2016a, MNRAS, 456, 1723
 Li J.-T., Bregman J. N., Wang Q. D., Crain R. A., Anderson M. E., 2016b, ApJ, 830, 134
 Li J.-T., Bregman J. N., Wang Q. D., Crain R. A., Anderson M. E., Zhang S., 2017, ApJS, 233, 20
 Li J.-T., Bregman J. N., Wang Q. D., Crain R. A., Anderson M. E., 2018, ApJL, 855, 24
 Liu J., Mao S., Wang Q. D., 2011, MNRASL, 415, 64
 Liu J., Wang Q. D., Mao S., 2012, MNRAS, 420, 3389
 McCammon D., Cryogenic Particle Detection, Topics in Applied Physics, v99. Springer-Verlag Berlin/Heidelberg, 2005, p1
 Miller M. J., Bregman J. N., 2015, ApJ, 800, 14
 Mineo S., Gilfanov M., Lehmer B. D., Morrison G. E., Sunyaev R., 2014, MNRAS, 437, 1698
 Mora-Partiarroyo S. C., Krause M., Basu A., et al., 2019, submitted to A&A
 O’Sullivan E., Ponman T. J., Collins R. S., 2003, MNRAS, 340, 1375
 Otte B., Murphy E. M., Howk J. C., Wang Q. D., Oegerle W. R., Sembach K. R., 2003, ApJ, 591, 821
 Ranalli P., Comastri A., Origlia L., Maiolino R., 2008, MNRAS, 386, 1464
 Rasmussen J., Sommer-Larsen J., Pedersen K., Toft S., Benson A., Bower R. G., Grove L. F., 2009, ApJ, 697, 79
 Revnivtsev M., Sazonov S., Churazov E., Forman W., Vikhlinin A., Sunyaev R., 2009, Nature, 458, 1142
 Smith R. K., Foster A. R., Brickhouse N. S., 2012, AN, 333, 301
 Strickland D. K., Heckman T. M., Weaver K. A., Hoopes C. G., Dahlem M., 2002, ApJ, 568, 689
 Strickland D. K., Heckman T. M., Colbert E. J. M., Hoopes C. G., Weaver K. A., 2004a, ApJS, 151, 193
 Strickland D. K., Heckman T. M., Colbert E. J. M., Hoopes C. G., Weaver K. A., 2004b, ApJ, 606, 829
 Strickland D. K., Heckman T. M., 2007, ApJ, 658, 258
 Strickland D. K., Heckman T. M., 2009, ApJ, 697, 2030
 Strong A. W., Porter T. A., Digel S. W., et al., 2010, ApJL, 722, 58
 Sun M., Voit G. M., Donahue M., et al., 2009, ApJ, 693, 1142
 Tang S. K., Wang Q. D., Lu Y., Mo H. J., 2009, MNRAS, 392, 77
 Toft S., Rasmussen J., Sommer-Larsen J., Pedersen K., 2002, MNRAS, 335, 799
 Tüllmann R., Pietsch W., Rossa J., Breitschwerdt D., Dettmar R.-J., 2006a, A&A, 448, 43

Tüllmann R., Breitschwerdt D., Rossa J., Pietsch W., Dettmar R.-J.,
2006b, *A&A*, 457, 779
Vikhlinin A., Kravtsov A., Forman W., et al., 2006, *ApJ*, 640, 691
Wang Q. D., 2010, *PNAS*, 107, 7168
Wang Q. D., Li J., Jiang X., Fang T., 2016, *MNRAS*, 457, 1385
Yamada S., Ohashi T., Ishisaki Y., et al., 2018, *JLTP*, 193, 1016
Zhang S., Wang Q. D., Ji L., Smith R. K., Foster A. R., Zhou X., 2014,
ApJ, 794, 61

